International Journal of New Technology and Research (IJNTR)
ISSN: 2454-4116, Volume-4, Issue-6, June 2018 Pages 25-41

Acoustic (Ultrasonic) Non-Diffracting Beams: Some Theory, and *Proposals of Acoustic Antennas* for Several Purposes

Michel Zamboni-Rached, Erasmo Recami*

***Abstract*— On the basis of a suitable theoretical ground, we study and propose Antennas for the generation, in Acoustics, of Non-Diffracting Beams of ultrasound. We consider for instance a frequency of about 40 kHz, and foresee fair results even for finite apertures endowed with reasonable diameters (e.g., of 1 m), having in mind various possible applications, including remote sensing. We then discuss the production in lossy media of ultrasonic beams resisting both diffraction and attenuation. Everything is afterward examined even for the cases in which high-power acoustic transducers are needed (for instance, for detection at a distance —or even explosion— of buried objects, like Mines).**

***Index Terms*—Acoustic Non-Diffracting Beams; Truncated Beams of Ultrasound; Remote sensing; Diffraction, Attenuation, Annular transducers, Bessel beam superposition, Beams resisting diffraction and attenuation, Acoustic Frozen Waves, Detection of buried objects, Explosion of Mines at a distance.**

I. INTRODUCTION

In this paper we present work on theory and generation, in Acoustics, of Non-Diffracting Beams[1,2]of ultrasound; having in mind various possible applications, including remote sensing (we shall leave aside, however, the "Acoustic Frozen Waves", which have been already investigated elsewere [3,4]).

Acoustic Non-Diffracting Waves (ANDW) were first studied, generated, and applied by Lu *et al.*, starting in 1992, for the particular case of the so-called (ultrasonic) X-shaped waves (see, e.g., Refs.[5,6]). For reviews about Non-Diffracting Waves (NDW), including X-shaped waves (as well as the mentioned Frozen Waves), one can see for instance Refs.[7,8], besides the initial Chapters in the already quoted books [1,2].

The NDWs, including of course the ANDWs, arose interest because of their spatio-temporal localization, unidirectionality, soliton-like nature, and self-healing properties[1,2]: All of them bearing interesting consequences, from theoretical and experimental points of view, in all sectors of physics in which a role is played by a wave equation. The NDWs would keep such properties all along an infinite distance, only in the ideal case of unlimited antennas, implying an infinite energy flux through any transverse plane. Such ideal NDWs cannot be practically generated, of course; and careful work was needed for finding out analytic expressions for realistic NDWs –for example *truncated*—, and afterward producing them (see Refs.[9,10] and refs. therein). Any realistic, finite-energy NDW will maintain its good properties only within a certain depth of field: much longer, however, than the one reached by a diffracting wave like the gaussian ones[1,2].

Let us first consider the problem of the truncated pulses *in general* (in electromagnetism, say), before passing to Acoustics.

A. *Analytic Expressions for Truncated Non-Diffracting Pulses*

Let us go on, therefore, to the problem of constructing in analytic form truncated Non-Diffracting Waves, in order to be more easily able to produce them experimentally. We address here the case of *pulses*, since the case of beams have been exploited elsewhere (see, e.g., Refs.[9,10] and refs. therein).

When one truncates an ideal non-diffracting pulse (INDP), the resulting wave field cannot be obtained, in general, in analytic form. One has to resort, in such cases, to the diffraction theory and perform numerical evaluations of the diffraction integrals, such as that, well known, of Rayleigh-Sommerfeld. And, indeed, one can get important pieces of information about a truncated non-diffracting pulse (TNDP) by performing numerical simulations of its longitudinal evolution, especially when the pulse is axially symmetric.

However, let us stress first of all the possibility of obtaining truncated non-diffracting pulses in analytic form even by a heuristic method. Subsequently, we are going to show how the solutions forwarded by an efficient method, expounded in Ref.[9] for *beams*, can be transformed into closed form expressions for truncated non-diffracting *pulses*[11].

B. *A heuristic approach*

First of all, let us recall that a preliminary method for describing the on-axis space-time evolution of truncated non-diffracting pulses, be they subluminal, luminal or superluminal, was developed in Ref.[12]. Within the framework of that quite simple method, the on-axis evolution

Michel Zamboni-Rached, DECOM, FEEC, UniversidadeEstadual de Campinas (UNICAMP), Campinas, SP, Brazil
Photonics Group, Electrical & Computer Engineering, University of Toronto, CA.
Erasmo Recami, DECOM, FEEC, Universidade Estadual de Campinas (UNICAMP), Campinas, SP, Brazil
Facoltà di Ingegneria, Università statale di Bergamo, Bergamo, Italy.
INFN—Sezione di Milano, Milan, Italy
(*) Corresponding author: "Bolsista CAPES/BRASIL": Supported as a Visiting Professor c/o UNICAMP by a PVE Fellowship of CAPES/BRAZIL

of a TNDP depends only on the frequency spectrum $S(\omega)$ of the corresponding INDP, Ψ_{INDP} ; in contrast to the Rayleigh-Sommerfeld formula which depends on the explicit mathematical expression of Ψ_{INDP} . Such a heuristic method, due to its simplicity, can yield closed-form expressions which describe the on-axis evolution of innumerable TNDPs. In Ref.[12] one can find the analytic expressions for the truncated versions of several well-known localized pulses: subluminal, luminal, or superluminal. Therein, the theoretical results were compared with those obtained through the numerical evaluations of Rayleigh-Sommerfeld integrals, with excellent agreement. Here, we confine ourselves just to present an example of such noticeable agreements, by Figures 1 and 2.

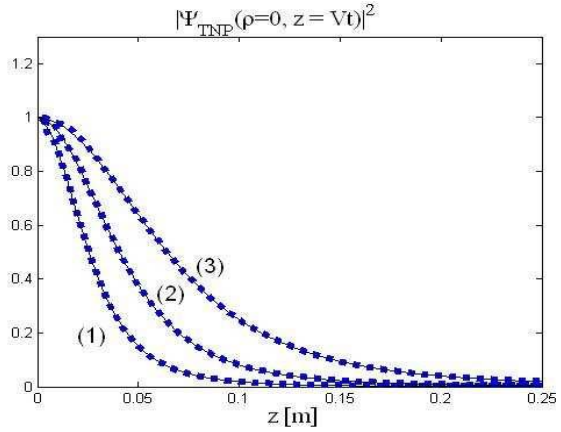

Figure 1: (Color online) Peak intensity evolution of a subluminal TNDP for three choices[12] of the parameters [(1) $V = 0.995c$ and $b = 1.5\times10^{15}$ Hz; (2) $V = 0.998c$ and $b = 6\times10^{14}$ Hz; (3) $V = 0.9992c$ and $b = 2.4\times10^{14}$ Hz]. In all cases the aperture radius is $R = 4$ mm. Remember thelinear relation $\omega = Vk_z + b$. The continuous lines are obtained from the closed-form analytic expression (eq.23 in Ref.[12]), while those represented by dotted lines come from the numerical simulation of the Rayleigh-Sommerfeld formula (eq.8 in [12]). Theagreement is excellent: Practically, no difference is perceivable.

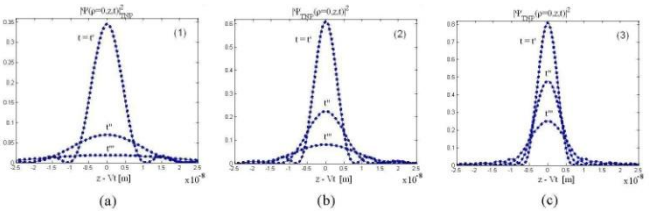

Figure 2: (Color online) On-axis evolution of the same subluminal TNDP considered in Fig.1, at three different instants of time [$t' = 0.11$ ns, $t'' = 0.22$ ns and $t''' = 0.33$ ns]. Figures a, b and c represent the cases (1),(2) and (3) respectively. The continuous lines are the results obtained fromthe closed-form expression, while those represented by dotted lines come from the numerical simulation of the Rayleigh-Sommerfeld formula. Again, the agreement is excellent: No difference is detectable.

The mentioned approach in [12] is actually useful, because in general it furnishes closed-form analytic expressions avoiding the need of time-consuming numerical simulations; and also because those closed-form formulae provide an efficient tool for exploring several properties of the truncated localized pulses: as their depth of field, longitudinal pulse behavior, decaying rates, etc.

However, let us turn to a more rigorous approach.

C. Again on closed-forms for Non-Diffracting Pulses, in the Fresnel regime, generated by finite apertures

Let us fix our attention to the method developed in [9], that we shall call for brevity “the MRB method"; it can be found summarized, now, also in [13]. By that method, the analytic description was obtained of some monochromatic waves: namely, of a few (important) beams generated by finite apertures. The important point is that one can generalize the efficient method MRB, in the paraxial approximation, for the case of *pulses*.

Since we are going to use superpositions of Bessel-Gauss beams, let us start by recalling the form of the so-called Bessel-Gauss beam[14]:

$$\Psi_{BG}(\rho,z) = -\frac{ikA}{2zQ} e^{ik\left(z+\frac{\rho^2}{2z}\right)} J_0\left(\frac{ikk_\rho\rho}{2zQ}\right) e^{-\frac{1}{4Q}\left(k_\rho^2+\frac{k^2\rho^2}{z^2}\right)}, \quad (1)$$

which appears to be a Bessel beam transversally modulated by the Gaussian function. Quantity $Q = q - ik/2z$, and k_ρ (the transverse wavenumber associated with the modulated Bessel beam) is a constant. [When k_ρ = 0, the Bessel-Gauss beam results in the well-known Gaussian beam. The Gaussian beam, and Bessel-Gauss, Eq.(10), are among the few solutions to the Fresnel diffraction integral that can be obtained analytically]. The situation gets much more complicated, however, when facing beams truncated in space by finite circular apertures: For instance, a Gaussian beam, or a Bessel beam, or a Bessel-Gauss beam, truncated via an aperture with radius R . [In this case, the upper limit of the Fresnell integral becomes the aperture radius, and the analytic integration becomes very difficult, requiring recourse, as we were saying, to lengthy numerical calculations]. Afterward, let us also recall that –in the case of beams– we considered the solution given by the following superposition of Bessel-Gauss beams:

$$\Psi(\rho,z) = -\frac{ik}{2z} e^{ik\left(z+\frac{\rho^2}{2z}\right)} \sum_{n=-N}^{N} \frac{A_n}{Q_n} J_0\left(\frac{ikk_\rho\rho}{2zQ_n}\right) e^{-\frac{1}{4Q_n}\left(k_\rho^2+\frac{k^2\rho^2}{z^2}\right)}, \quad (2)$$

quantities A_n being constants, and Q_n being given by $Q_n = q_n - \frac{ik}{2z}$, where the q_n are constants that can assume complex values. In this superposition all beams possessed the same value of k_ρ . In our previous work, we wanted the solution (2) to be able to represent beams truncated by

circular apertures, in the case of Bessel beams, gaussian beams, Bessel-Gauss beams, and plane waves. And, given one of such beams, truncated at $z=0$ by an aperture with radius R, we determined the coefficients A_n and q_n in such a way that Eq.(2) represented with fidelity the resulting beam. More details can be found in the papers of ours quoted above.

Let us recall, before going on, that in previous work we found an equation which could be used for representing, on the plane $z=0$, truncated Gaussian, Bessel, Bessel-Gauss beams and truncated Plane waves; with the consequence that the evolution of such truncated beams was given by Eq.(2). *The interesting question, for us, is now: Is it possible to derive from what precedes also analytic descriptions of* pulses truncated *by finite apertures?:* For instance, for TBP (truncated Bessel pulses), TBGP (truncated Bessel-Gauss pulses), TGP (truncated gaussian pulses), and TPP (truncated plane-wave pulses)? [even if we shall fix our attention only on truncated Bessel pulses]. We shall answer this question within the paraxial approximation; to this aim, consider an envelope $\psi(x,y,z;t)$ obeying[23] the equation of the paraxial waves

$$i[\partial\psi/\partial z+(1/c)\partial\psi/\partial t]-(1/2k)\nabla_{\perp}{}^{2}\psi=0\,, \quad (3)$$

where the time dependence of ψ is essential [and cannot be eliminated as in the case of beams]. When assuming axial symmetry, one can write

$$\psi(\rho,z,t)=\int_0^{\infty}dk_{\rho}\int_{-\infty}^{\infty}duS(k_{\rho},u)J_0(k_{\rho}\rho)\,e^{iuz/c}\,e^{-i(k_{\rho}^2/2k_o)z}\,e^{-iut}\,, \quad (4)$$

where we replaced ω with the variable u (since $\omega\equiv\omega_0$ will mean here the pulse central frequency). As usual, it is $k\equiv\omega c$, and $k_z=u/c-k_{\rho}^2/k_o$. If we know $\psi(\rho,z,t)$ *on the plane* $z=0$ *of the aperture*, it will be

$$\psi(\rho,0,t)=\int_0^{\infty}dk_{\rho}k_{\rho}\int_{-\infty}^{\infty}duS(k_{\rho},u)J_0(k_{\rho}\rho)\,e^{-iut}\,, \quad (5)$$

in terms of one Fourier-Bessel and one Fourier transformation. By using the corresponding inverse transformations, one succeeds in writing the spectral function $S(k_{\rho},u)$ as a function of the field existing at the aperture!; namely

$$S(k_{\rho},u)=(1/2\pi)\int_0^{\infty}d\rho\rho\int_{-\infty}^{\infty}dtJ_0(k_{\rho}\rho)\,e^{iut}\,\psi(\rho,0,t)\,. \quad (6)$$

Inserting Eq.(6) into Eq.(4), and reversing the order of the integrations over k_{ρ} and u, one gets

$$\psi(\rho,z,t)=\int_0^{\infty}d\rho'\int_0^{\infty}dt'$$

$$\times\left\{\rho'\psi(\rho',0,t')\left[\int_0^{\infty}dk_{\rho}k_{\rho}J_0(k_{\rho}\rho)J_0(k_{\rho}\rho')e^{-i(k_{\rho}^2/2k_o)z}\right]\left[\int_{-\infty}^{\infty}due^{iu(z-ct)/c}e^{iut'}\right]\right\}. \quad (7)$$

The last part in square brackets yields the Dirac delta $2\pi\delta(z+ct'-ct)$. With some more algebra, one reaches the equation

$$\psi(\rho,z,t)=\int_0^{\infty}d\rho'\int_0^{\infty}dt'\{\rho'\psi(\rho',0,t')$$

$$\times\left[(k_o/z)\exp\left[i(k_o/4z)(\rho^2+\rho'^2)\right]J_0\left(k_o\rho\rho'/z\right)\right]\left[\delta\left(z+ct'-ct\right)\right]\}\,, \quad (8)$$

which can be finally integrated over t', without difficulties due to the presence of the delta, *furnishing for a pulse the solution we were looking for:*

$$\psi(\rho,z,t)=\int_0^{\infty}d\rho'\rho'\,\psi\left(\rho',0,z-ct\right)(k_o/z)\exp[ik_o(\rho^2+\rho'^2)/(4z)]e^{ik\rho'^2 2z}\,J_0\left(k_o\rho\rho'/z\right), \quad (9)$$

where one can notice that under the integral it now appears quantity $(z-ct)$ instead of t. Equation (9) is the analogous of the one found out by our MRB method for beams.

The integral solution (9) tells us that the pulsed field (envelope) can be obtained by merely knowing its value in the plane $z=0$ *of the aperture, as a function of time and of the spatial coordinate.* The result in Eq.(9) is interesting also because it extends the MRB method to pulsed fields: In the sense that one can utilize any solution found by the said method[9] for beams, transforming it into a solution for pulses via a mere multiplication by the function $\exp[-(z-ct^2)/(c^2T^2)]$. More precisely:

—to get a truncated beam, it is enough to have at the aperture a field of the type $\psi(\rho,0) \approx J_0(k_\rho \rho)\, circ(\rho/R)$;

—to get a truncated pulse, it will be enough to have at $z=0$ an analogous field of the type $\psi(\rho,0,t) \approx J_0(k_\rho \rho)\exp(-t^2/T^2)\, circ(\rho/R)$;

where the multiplying function $\exp[-(z-ct^2)/(c^2T^2)]$ reduced to $\exp(-t^2/T^2)$ on supposing that $T >> 2\pi/\omega$. One can also notice that, having recourse to multiplying functions of the type $\exp[-(t/T)^{2n}]$, one can get a series of (for instance) step-shaped pulses.

II. Applications for Acoustic (Ultrasonic) Non-Diffracting Pulses

Let us finally consider ultrasonic (acoustic) pulses, for instance with a central frequency of 40 kHz, generated by a finite aperture with radius $R = 0.5$ m. One may have in mind, for example, remote sensing, and the purpose of obtaining a realistic pulse which keeps its spot-size unvaried for, say, 20 m. We shall apply of course the results of our last subsection, which allow us to describe analytically several truncated pulses without any need, again, of lengthy numerical simulations.

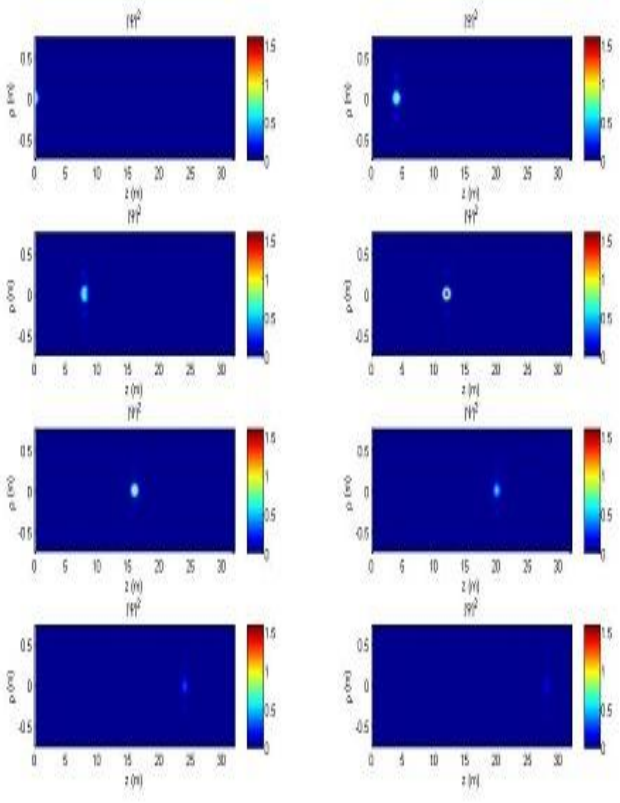

Figure 3: (Color online) As an application of our last method to ultrasonic (acoustic) pulses, let us consider a truncated Bessel pulse with initial spot-radius of 15 cm, generated by a finite antenna with radius $R = 0.5$ m. Attenuation (actually strong in the air when its central frequency is assumed to be 40 kHz) is neglected here. If one has in mind, for example, remote sensing, he may want our realistic pulse to keep its spot size unvaried for, say, 20 m. The present set of figures, representing by colors the actual pulse evolution, does indeed show such abehavior.

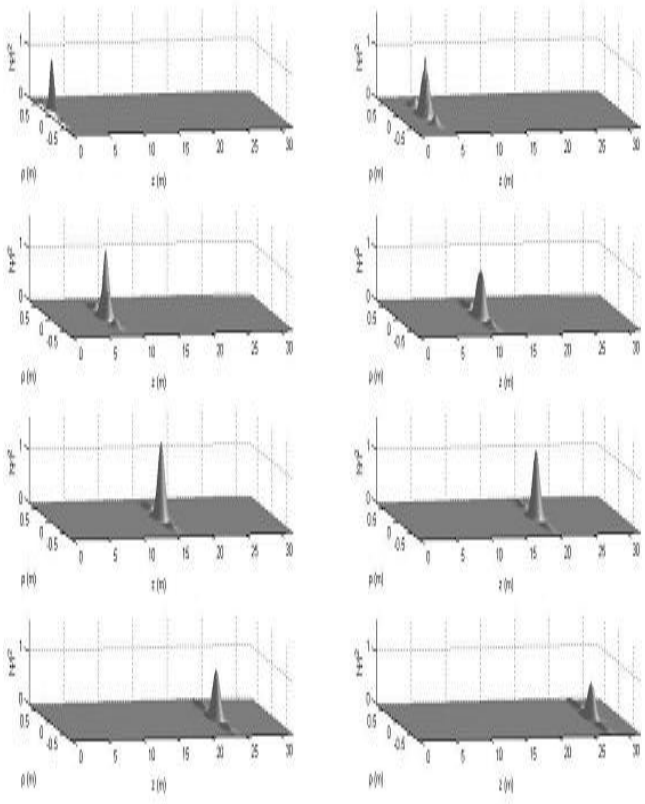

Figure 4: This second set of figures shows, in terms of 3D plots, the evolutions of the same truncated Bessel pulse considered in the previous Figure. In this case, the intensity is given by the height of $|\psi|^2$. From these figures one can easily see the pulse spot (initially with a radius of 15 cm) to keep rather well its size for about 20 m, just with an oscillating intensity due to the edge-effects of the finite antenna. Afterward, the pulse strongly deteriorates; and, to get better results by a Bessel pulse like this, one ought to use larger antennas.

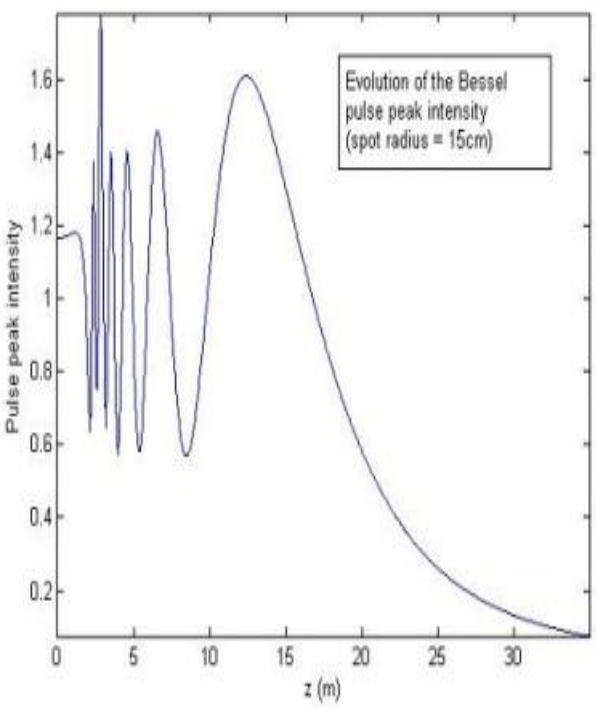

Figure 5: (Color online) In this further figure we depict the evolution, during propagation, of the intensity peak of the same truncated Bessel pulse; still keeping no account of attenuation.

We shall confine ourselves, however, to just a few examples. Let us start with a truncated Bessel pulse with a spot-radius of 15 cm. For simplicity, we shall not take here into account the pulse attenuation, quite present for the said frequency in the air, even if one could take account of it without too much difficulty.

Such a Bessel pulse, a priori, can be easily generated. If we think in terms of a simple antenna, constituted by an array of annular transducers, then: (i) transducers do exist working with the mentioned frequency; (ii) amplitudes and phases of the vibrations are given as functions of the chosen pulse; (iii) the pulsed excitation (a modulation of the carrier wave) is the same for all transducers, and we choose precisely a temporal gaussian with $\Delta t = 2.5$ ms, hundred times larger than the period of the 40 kHz wave ($T = 2.5\,x10^{-5}$ s). Incidentally, the choice of pulses with duration much longer than the carrier period is requested by the slow-envelope approximation, assumed by us when generalizing the MRB method for pulses.

Let us give an idea of the results by the help of suitable Figures.

The first set of figures, Fig.3, shows the pulse evolution by colors. By contrast, the second set of figures, Fig.4, shows it in terms of 3D plots (the intensity being represented by the eigthof $|\psi|^2$). From figures 4 one can clearly see the pulse spot (initially with a radius of 15 cm) to keep rather well its size for about 20 m, just with an oscillating intensity due to the edge-effects of the finite antenna. Afterward, the pulse strongly deteriorates; and, to get better results by such a Bessel pulse, one ought to use larger antennas.

By the the last figure, Fig.5, we depict the evolution of its intensity peak while propagating (still keeping no account of the attenuation).

A. *Further Cases*

Second case: Truncated Bessel beam with a spot radius of 23 cm

Suppose we want to get now a spot keeping its size for a larger distance, arriving at about thirty meters; while the radius of the generating antenna remains $R = 0.5$ m.

As before, the pulse evolutions is first shown by colors (Fig.6), and then in terms of 3D plots (Fig.7), when the intensity is represented by the height of $|\psi|^2$.

One can see that the impulse spot radius (initially of 23 cm) maintains its value for about 30 m, oscillating in intensity due to the edge effects of the finite antenna. Afterward, the pulse strongly deteriorates; once more, to get better results by a Bessel pulse like this, one ought to use larger antennas.

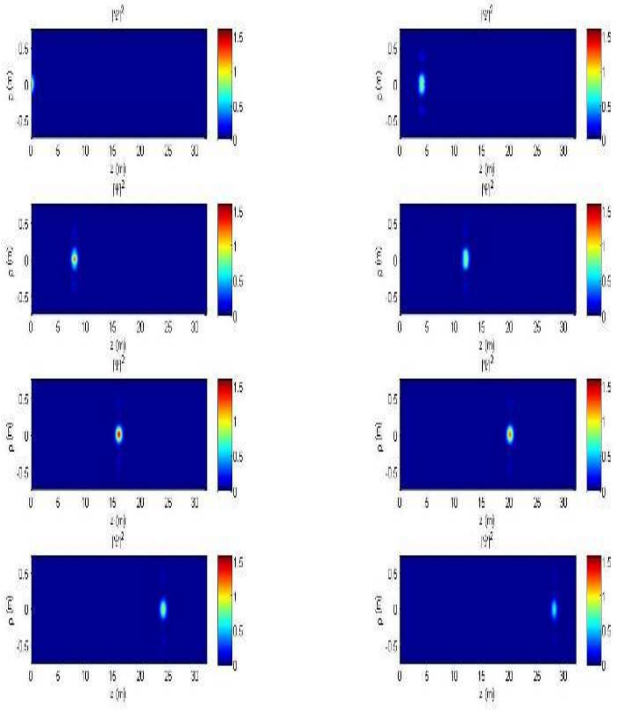

Figure 6: (Color online) As a second application of our method to ultrasonic (acoustic) pulses, let us consider now a truncated Bessel pulse with an initial spot-radius of 23 cm, generated by a finite antenna still with radius $R = 0.5$ m. Attenuation (actually strong for a 40 kHz frequency) is neglected again. We wanted our realistic pulse to keep its spot size unvaried for the larger distance of about 30 m. The present set of figures, representing by colors the actual pulse evolution, does indeed show such a behavior.

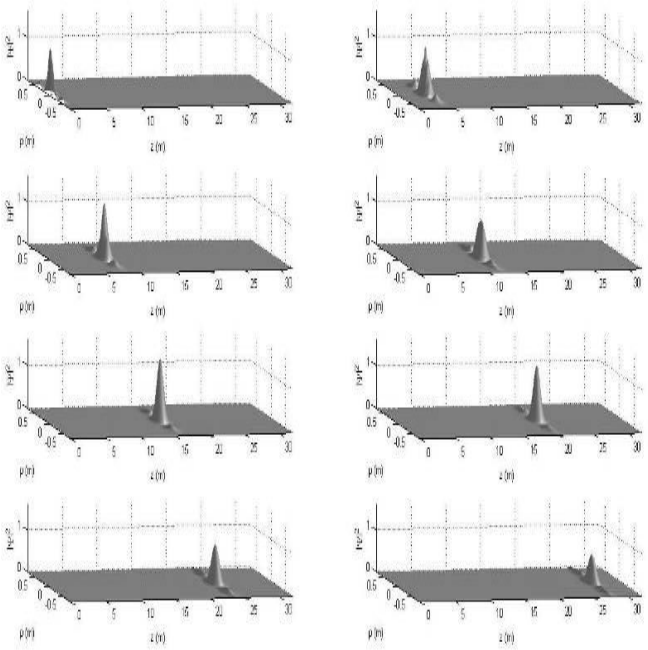

Figure 7: This second set of figures shows, in terms of 3D plots, the evolutions of the same truncated Bessel pulse considered in the previous Figure (its intensity being now the height of $|\psi|^2$). From the present figures one can see even better that the pulse spot (initially with a radius of 23 cm) keeps rather well its size for almost 30 m. Afterward, the pulse strongly deteriorates; and, to get better results by a Bessel pulse like this, one has once more to use larger antennas.

By the the last figure, Fig.8, we depict the evolution of its intensity peak while propagating (when attenuation is neglected).

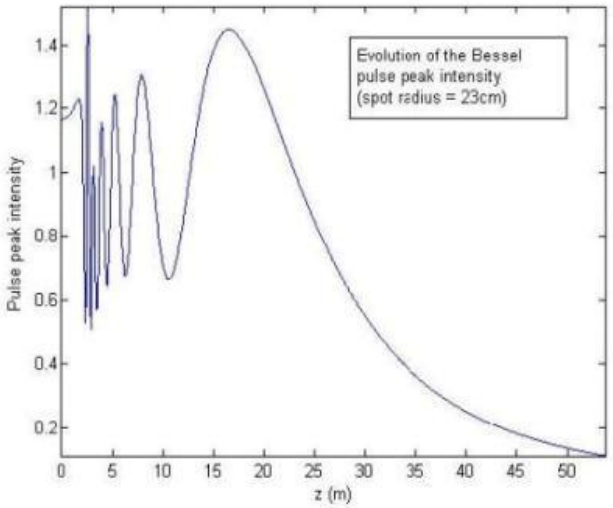

Figure 8: (Color online) In this further figure we depict the evolution, during propagation, of the intensity peak of the same truncated Bessel pulse.

Third case: Truncated Plane Wave Pulse

The first set of figures, Fig.9, shows the pulse evolution by colors; the second set, Fig.10, shows it by 3D plots (the pulse intensity being the height of $|psi|^2$).

In this case one clearly recognizes the interesting fact that the initial spot-radius, of 0.5 m, changes during propagation *diminishing* during the first 30 meters till 0.3 m. After such a distance, however, the pulse starts to open: and its spot-size increases.

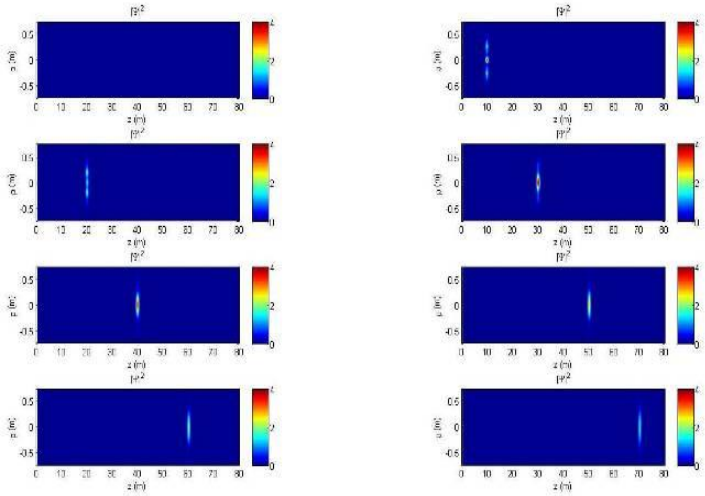

Figure 9: (Color online) As a third application of our method to ultrasonic (acoustic) pulses, let us now consider a Truncated Plane Wave Pulse, with initial spot-radius of 0.5 m. It is interesting that the spot size does *diminish* during propagation, till a distance of 30 m. Only afterward, it start increasing, and the pulse opens. The present set of figures shown such a behavior by colors.

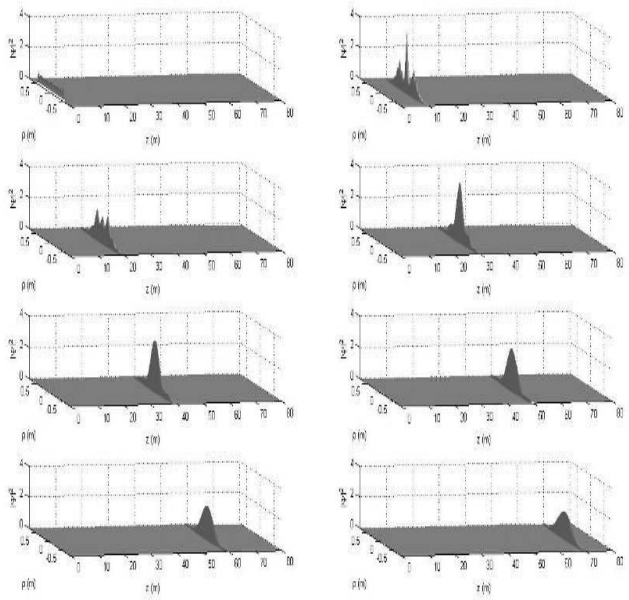

Figure 10: This second set of figures shows, in terms of 3D plots, the evolutions of the Truncated Plane Wave Pulse considered in the previous Figure.From the present figures one can see even better that the pulse spot (initially with a radius of 0.5 m) *reduces* its size for almost 30 m, reaching the value of 0.3 m. Only afterward the pulse opens (its spot-size increasing).

By the the last figure, Fig.11, we depict the evolution of its intensity peak while propagating (when attenuation is neglected).

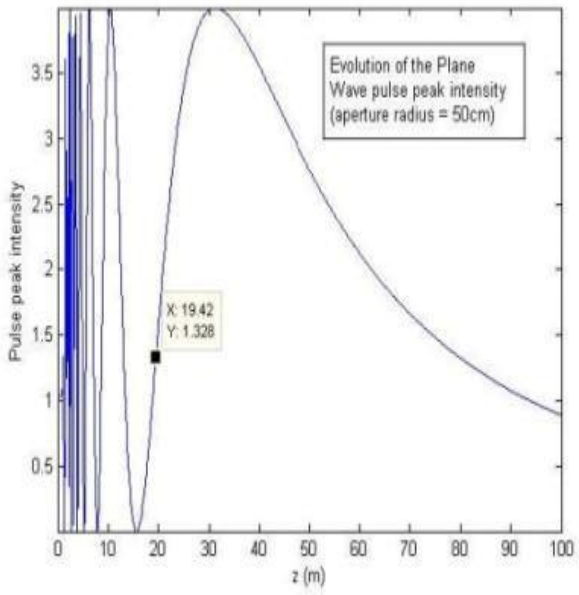

Figure 11: (Color online) In this further figure we depict the evolution, during propagation, of the intensity peak of the same Plane Wave truncated pulse.

Fourth case: Pulse of Plane Wave Truncated and Focalized (at $z = 20$ m).

The first set of figures, Fig.12, shows the pulse evolution by colors; the second set, Fig.13, shows it by 3D plots (the pulse intensity being the height of $|psi|^2$).

In this case one can clearly see that a focalization takes place at $z = 20$ m. This quite interesting result has been obtained by having recourse to a Plane Wave truncated (and pulsed) at the aperture, and *modulated by a phase function similar to the transfer function of a convergent lens with a*20 m *focal distance*. The pulse leaves the antenna with a spot of 50 cm, which shrinks down (while the intensity increases), till reaching the distance of 20 m where the spot gets its minimum radius, of about 20 cm, and an intensity 20 times larger than the one at the aperture.

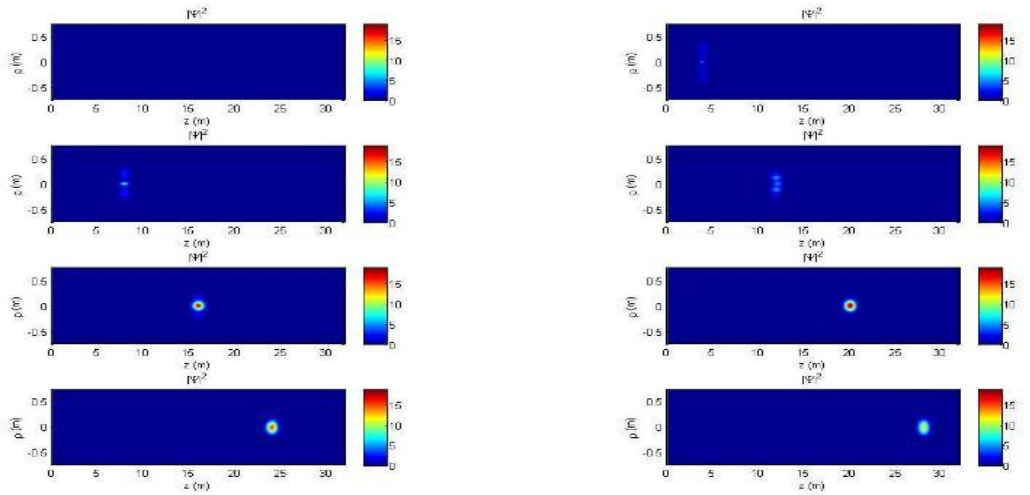

Figure 12: (Color online) As a third application of our method to ultrasonic (acoustic) pulses, let us now consider a Focalized Plane Wave (Truncated) Pulse, with initial spot-radius of 0.5 m. In this case a focalization takes place at $z = 20$ m. Such quite interesting result has been obtained by having recourse to a Plane Wave truncated (and pulsed) at the aperture, and modulated by a phase function similar to the transfer function of a convergent lens with a 20 m focal distance. The present set of figures show such a behavior by colors.

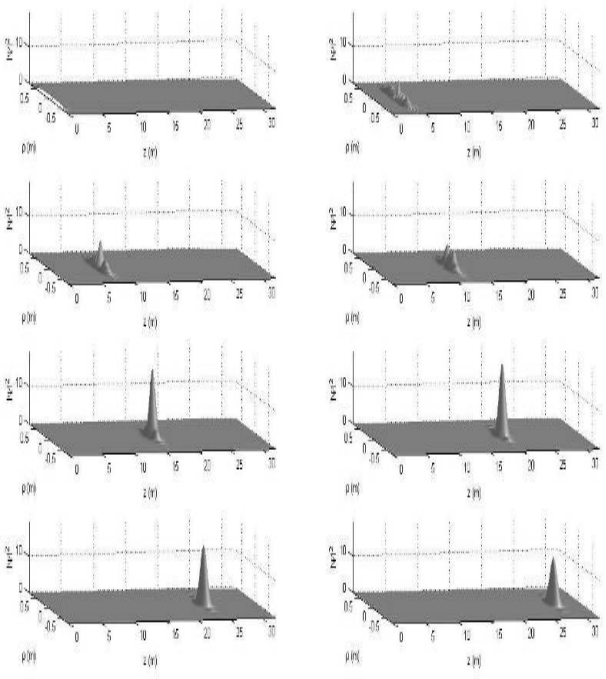

Figure 13: This second set of figures, in terms of 3D plots, shows the evolutions of the Focalized Plane Wave (Truncated) Pulse considered in the previous Figure. One can easily see that a focalization takes place at $z = 20$ m. This interesting result has been obtained —as we said– by having recourse to a Plane Wave truncated (and pulsed) at the aperture, and modulated by a phase function similar to the transfer function of a convergent lens with a 20 m focal distance. The pulse leaves the antenna with a spot of 50 cm, which shrinks down (while the intensity increases), till reaching the distance of 20 m where the spot gets its minimum radius, of about 20 cm, and an intensity 20 times larger than the one at the aperture.

By the the last figure, Fig.14, we depict the evolution of its intensity peak while propagating (when attenuation is neglected).

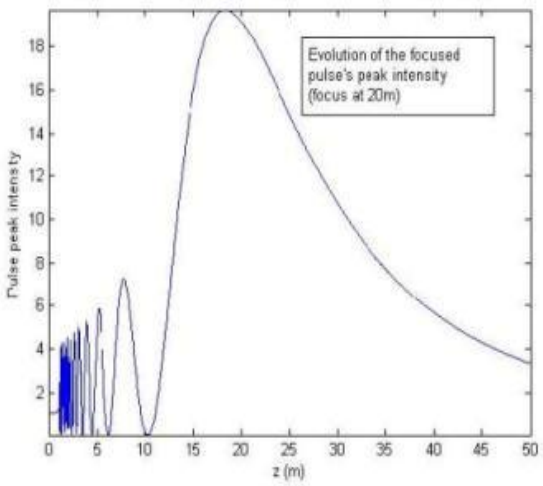

Figure 14: (Color online) In this further figure we depict the evolution, during propagation, of the peak of the same Focalized Plane Wave (Truncated) Pulse.

In the next Section we are going to propose acoustic (ultrasound) antennas suitable for detection (or explosion) of buried objects, like mines

III. Towards the Proposal of Acoustic Antennas for Detection (or Explosion) of Under-Ground Buried Objects, like Mines.

One of our main aims in this work is the proposal of antennas, producing Acoustic Localized Waves (better called ANDW = Acoustic Non-Diffracting Waves), for the detection of buried objects, like MINES, or for causing their explosion from a distance of at least 10 meters.

Let us recall, before all, that the Localized Waves are non-diffracting, and propagate in a single direction without deformation, with energy concentrated within a spot. Such good properties are kept for infinite times and lenghts, as we know, only by ideal beams; in the case of realistic beams, produced by finite antennas, those properties are maintained for a certain (finite, even if long) depth of field. Let us recall also the following: (i) the majority of the ANDWs considered in the literature are the "X-shaped" supersonic ones, initially produced in 1992 [6] in analogy to what had been theoretically predicted[15], and soon concretely utilized for an ultrasound scanner which directly furnishes 3D, high-resolution images of the human body[16], in particular of moving organs like the heart. (In the electromagnetic case, the X-shaped waves resulted to be endowed with superluminal peak-velocities, in hundreds of theoretical, mathematical, numerical-simulation, and experimental works[1,2]); (ii) Also investigated were Non-Diffracting Waves [NDW] with subluminal, in the electromagnetic case, and subsonic, in the acoustic case, peak-velocities; (iii) Particularly interesting they resulted to be the subluminal NDWs with zero peak-velocity: that is, with a static envelope (within which only the carrier wave propagates). They have been called *Frozen Waves* [FW], corresponding to electromagnetic, or acoustic, fields "at rest"[17]. The FWs can be created within the desired (even quite small) space region, with the chosen shape and intensity[18,19]. They are generated by superposing Bessel beams with the same frequency, which therefore can be prefixed too.

A. *Proposal of antennas creating AcousticFrozen Waves[AFW]*

Let us propose now the generation of *Acoustic Frozen Waves*, without forgetting that the air is an absorbing medium, especially for ultrasound waves.In the case of FWs we constructed a new theoretical *method* for their production, which allows to create the desided "static" field even in a lossy medium; in other words, it [20,21] allows *producing beams resisting both the effects of diffraction and attenuation.* For the reader's convenience, it will be summarized in the Appendix

Let us start by depicting how a single Bessel beam [Bb] behaves in an *absorbing* medium. For instance, let us consider an acoustic Bb of 100kHz, with an initial spot of 1.5cm. For such a frequency, the Bb is subject in air to an attenuation coefficient of 2dB per meter, and will thereforepossessa field depth of 2 meters only.The following

two figures, Figs.15, show such an effect for an isolated Bessel beam; the square magnitude $|\Psi|^2$ of its field intensity is shown in figure (a), as a function, besides of the transverse co-ordinate ρ, of the co-ordinate z along the propagation axis: Both co-ordinates being expressed in meters.Figure (b) depicts its orthogonal projection

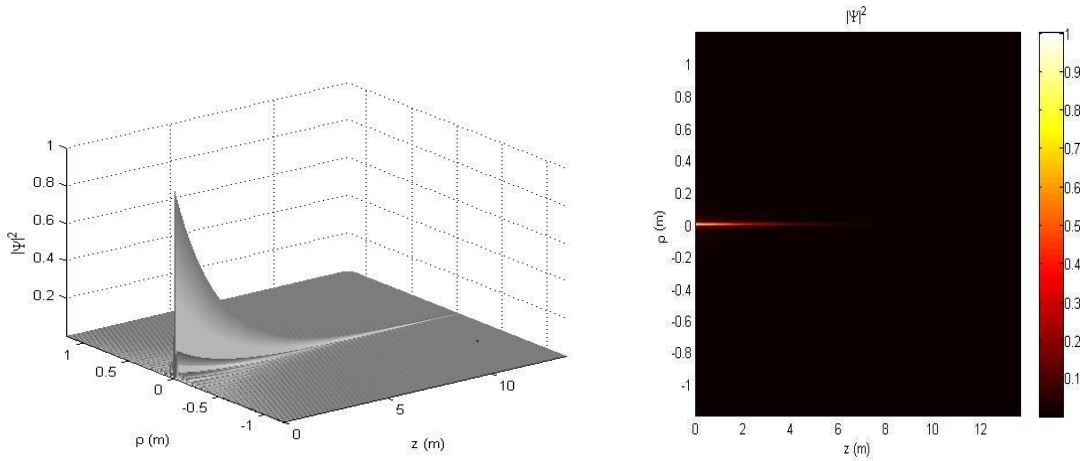

(15 a) (15 b)

Figs.15: The case of an isolated acoustic Bessel beam (100 kHz; spotof 1.5 cm), subject in air to strong attenuation (2 dB/m), so that its field depth is expected to be 2 m. Figure a): 3D behaviour of the field-intensity square-magnitude $|\Psi|^2$, as a function of (ρ and) z. Figure b): orthogonal projection.

First Example:

Let us choose a carrier frequency of 100kHz, in which case the attenuation in air is 2dB/m. For a normal beam (plane wave, or gaussian beam) the depth of field would be of 2.2m. We know that by suitable superposition of equal-frequency Bessel beams[20,2] we can obtain FWs resisting attenuation (besides diffraction).

The beam we want to obtain is a FW with a field depth of 11meters,the acoustic field being moreover concentrated, at that distance,so to build a spot of 3 cm. Our methodology[20,2] then suggests to be convenient an aperture of 0.9 m.Let us require the intensity longitudinal pattern of the FW equals a constant value over a rectangular region: we shall say it to be of a "double step"type[20] in the interval $0<z<11$m. More precisely, $\Psi(z)=1$ for $0< z <11$ m, and zero elsewhere.When having recourse to a superposition of a small number of Bb's, the results are ofthe type presented in Figs.16.

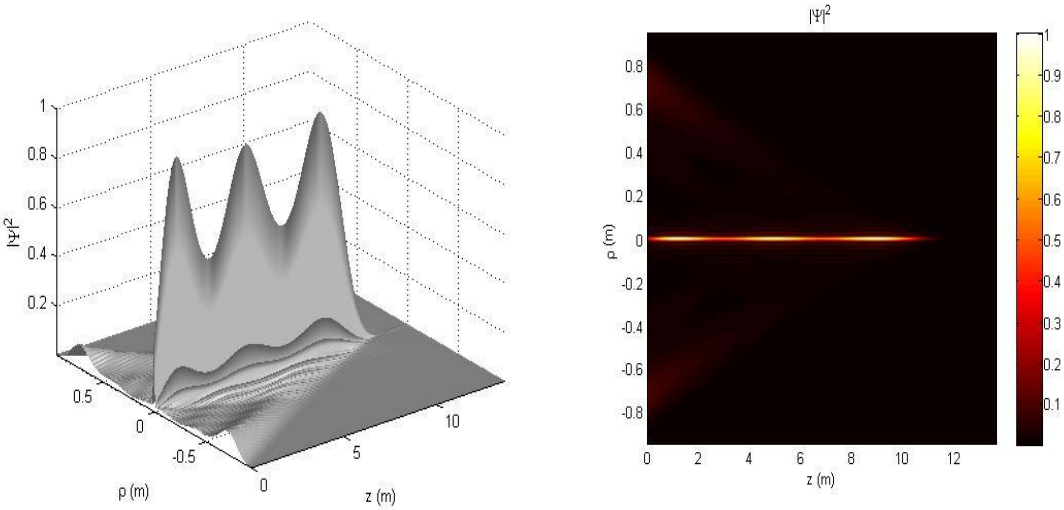

(16 a) (16b)

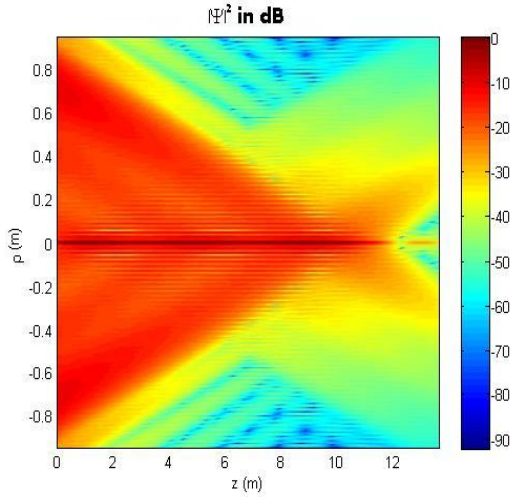

(16 c)

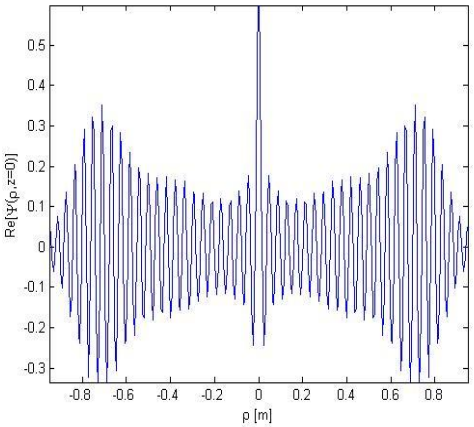

(16d)

Figs.16: (a) Intensity behaviour of the FW in the case of the First Example (a "double step" shape, with a small number of Bessel beams in the superposition); (b) Orthogonal projection;(c) Orthogonal projection by a logarithmic scale plot (i.e., in dB); d) Real part of the field at the aperture (z=0). As requested, the field depth results to be 11 m, with a spot radius of 0.3 m.

Second Example:

Let us consider a case analogous to the previous one (the longitudinal intensity shape being again of the "double step" type, in the interval 0< z <11 m), but aiming this time at obtaining the maximum precision allowed by the method, which implies in the present case a maximum number of 101 Bb's in the superposition[20]. Still, the frequency be 100 kHz, and the attenuation coefficient in air of 2 dB/m. Let us recall the depth of field of a normal beam (plane wave or gaussian beam) to be of 2.2 m. Our aim, once more, is getting a field depth of 11 m, with a spot diameter at that distance of 3 cm. We need an aperture of 0.9 m.The results, by the new superposition, are the ones in Figs.17.

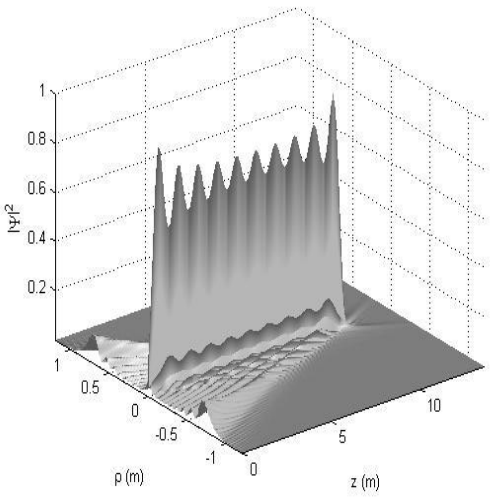

(17a)

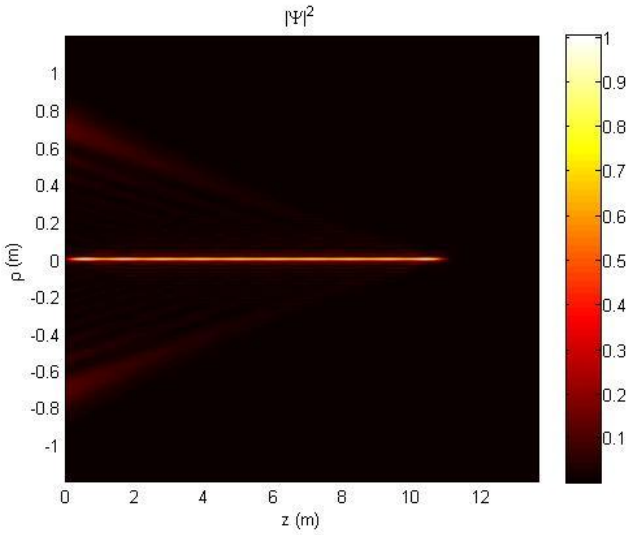

(17b)

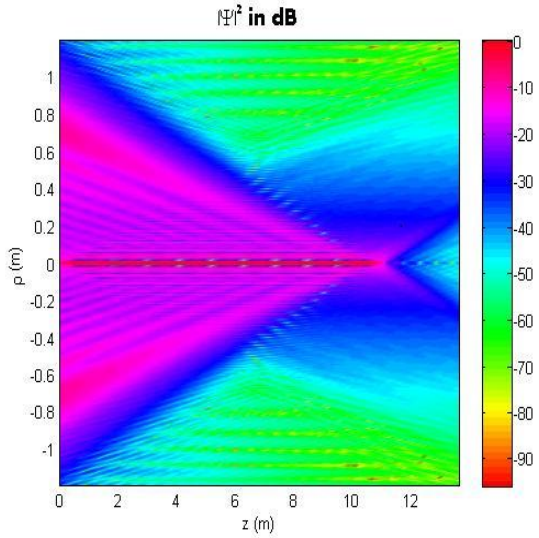

(17 c)

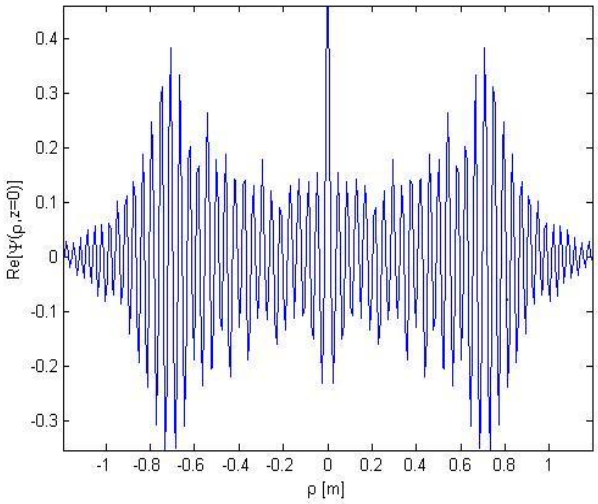

(17d)

Figs.17: (a) Intensity behaviour of the FW in the case of the Second Example (still a "double step" shape, but with the maximum allowed number of Bb's in the superposition); (b) Orthogonal projection; (c) Orthogonal projection by a logarithmic scale plot (i.e., in dB); d) Real part of the field at the aperture (z=0). As requested, the field depth results to be 11 m, with a spot radius of 0.3 m, but this time with the maximum precision allowed by the method.

Third Example:

Assume we wish now to get a FW with a depth of field of 20 meters. The needed aperture radius becomes now of 1.4 m. The longitudinal intensity shape be again a "double step", but in the interval 0< z <20 m. Obtaining a field depth of 20 m brings us close to the limits of validity of our method, but we can still reach good results. The intensity of the lateral converging beamswill increase, in order to reconstruct the resulting beam till a larger distance (20 m). The results appear in Figs.18.

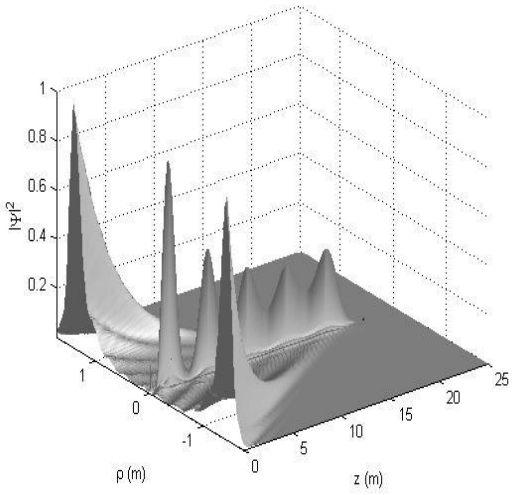

(18a)

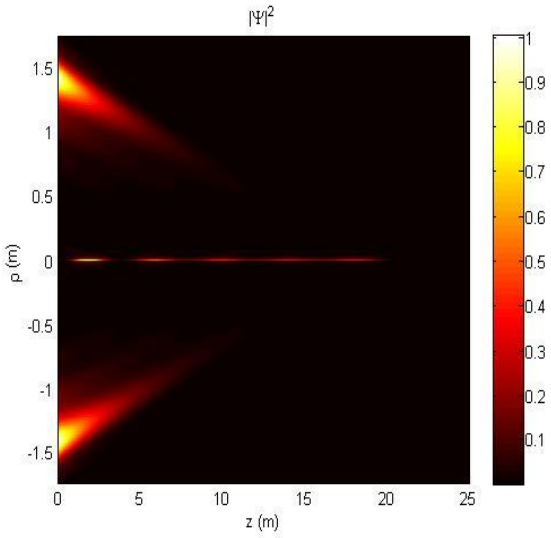

(18b)

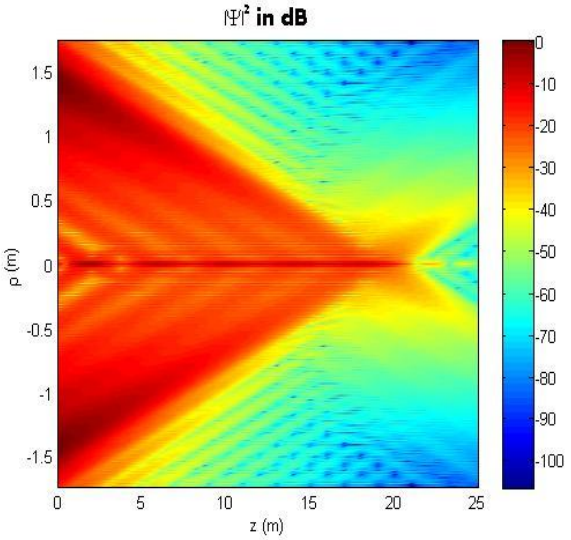

(18 c)(18 d)

Figs.18: These Figures illustrate the 3rd Example, referring this time to a FW with a depth of field of 20 meters. The needed aperture radius then becomes of 1.4 m. The longitudinal intensity shape is again a "double step", but in the interval 0< z <20 m. Requesting a field depth of 20 m brings us close to the limits of validity of our method, but we still reach good results. Figure (a): Intensity behaviour of the FW in the case of the Third Example; (b): Orthogonal projection; (c) Orthogonal projection by a logarithmic scale plot (i.e., in dB); d) Real part of the field at the aperture (z=0). As requested, the field depth results to be 20 m.

More material (equipped with suitable further Figures) will appear elsewhere.

IV. Some Considerations about Ultrasonic Transducers for Generating Non-Diffracting Beams or Pulses.

In this Section we are going to pay some preliminary attention to the construction of antennas for the generation of non-diffracting (or even ordinary) ultrasound beams, or pulses.

More specifically, we shall fix our attention --as before— to ultrasound beams resisting the effects of both diffraction and attenuation.

A. Introductory remarks

Before going on, let us *recall* that the use of non-diffracting ultrasound beams, or pulses, is already a reality in the realm of medical imaging. Well known are the applications of acoustic X-shapes waves for high resolution ultrasound scanning, by Jian-yu Lu. Our own research group has been proposing the adoption of the methods of the ultrasound Frozen Waves for modeling non-diffracting beams in lossy media: in order toapproach diverse applications, from imaging to remote sensing, and to curing tumours by killing the cancer cells via heating produced by extremely localized ultrasonic beams.

For instance in [1] and [2], we suggested arrays of annular concentric transducers to create very-high resolution ultrasonic FWs (cf. Figs.19-21). Figure 19 is an example of acoustic annular aperture, with radius 24.5 mm, and 41 rings (d = 0.5 mm; Δ_d=0.1 mm): specifically, it shows the section of an annular transducer array for constructing 1.5 MHz frozen waves. Using such an array, we shall attempt producing, in amplitude and phase, the field of the chosen FW at the antenna location, that is, in the plane z = 0.

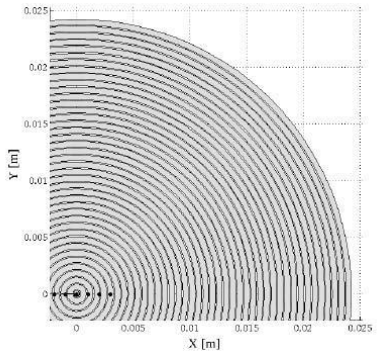

Fig. 19 – Example of an acoustic annular aperture having a radius of 24.5 mm and 41 rings (with width Δd=0.1 mm, and inter-ring distance d = 0.5 mm). The figure shows the section of the annular transducer array chosen for producing FWs of 1.5 MHz.

Before that, let us show (by Fig.20 and Fig.21) a sample of the excitation pattern (amplitude and phase, respectively) corresponding to the array in Fig.19: With R = 24.5 mm, Nr = 41, and f = 1.5 MHz. The average radii (in meters) of the emitting rings (transducers) appear on the horizontal axis.

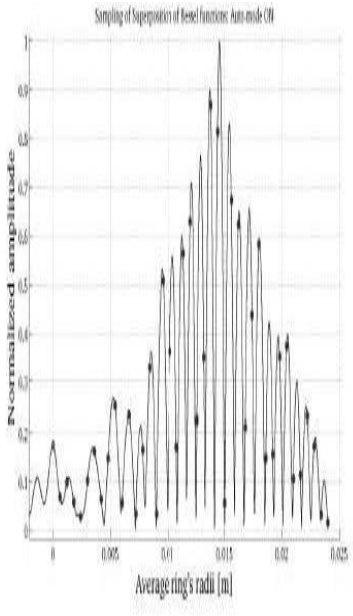

Fig. 20 – Amplitude pattern excited by the acoustic array in the previous Figure (radius of the array R = 24.5 mm; with 41emitting rings, and ultrasonic frequency f = 1.5 MHz). The values, in meters, on the horizontal axis represent the radii of the various emitting rings (transducers).

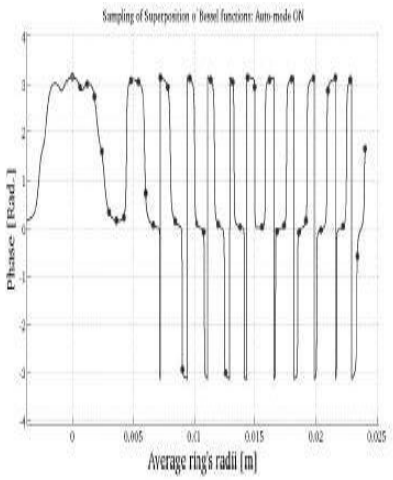

Fig. 21 – Pattern of the acoustic wave *phase* excited by the array in the previous Figure (that is, radius of the array *R* = 24.5 mm; with 41emitting rings, and ultrasonic frequency*f*= 1.5 MHz). The values, in meters, on the horizontal axis still represent the radii of the various emitting rings.

One should discretize the continuous field distribution at the aperture, as suggested and performed by us in [9], and in ref.[13], downloadable e.g. from http://arxiv.org/abs/1408.3635 , so that the annular transducers locations can be determined by such a discretization (see figures 7 and 12 therein).

Anyway, a possible set-up for the generation of FWs, when having recourse to an array of annular transducers, may be the one sketched in Fig.22.

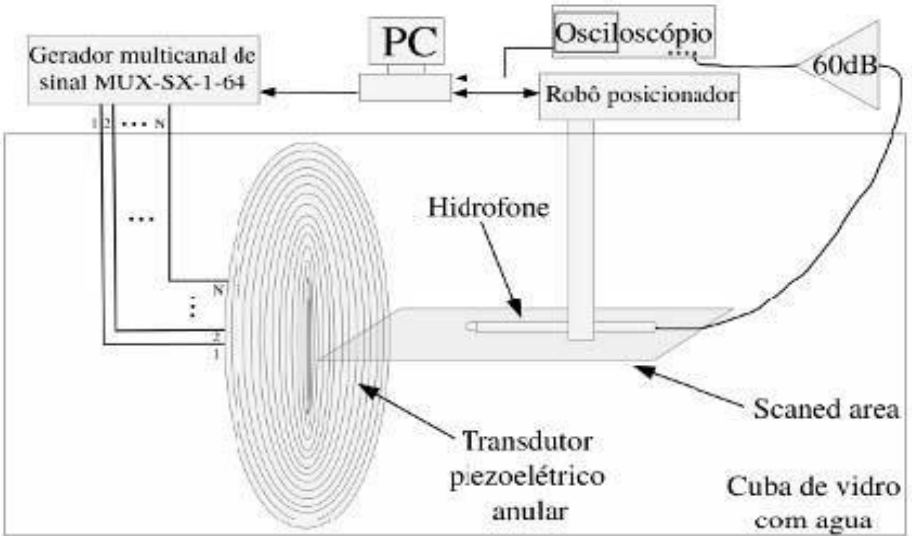

Fig. 22 – A possible experimental set-up for the creation of FWs, when having recourse to an array of annular transducers.

As a mere example, let us first forget about attenuation, and examine how a theoretical FW can be generated using an annular transducer antenna. One obtains the FW corresponding to the adopted array, by numerical simulation of the field emanated by it[3]. In the following Figures the values of z are in meters, while those of ρ are in mm.

Let us operate with f = 2.5 MHz, and L = 30 mm. The theoretical FW, to be experimentally constructed, is chosen to consist of two rectangular regions with different intensities; and to be expressible as the superposition of $2N+1$ = 25 Bessel beams. One thus obtains an highly concentrated ultrasonic beam, with a spot smaller that1 mm (near to the diffraction limit): as it is shown in our theoretical Fig.23.

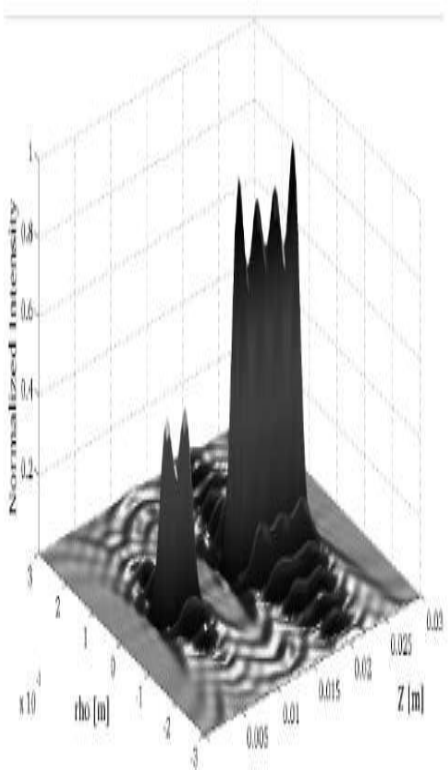

Fig. 23 – The theoretical FW we choose, for subsequent experimental creation, consists in two rectangular regions with different intensities; and is expressed as a superposition of $2N+1 = 25$ Bessel beams (we operate with $f = 2.5$ MHz, and $L = 30$ mm, neglecting attenuation: Cf. [3]). As depicted in this figure, one thus obtains a highly concentrated ultrasonic beam, with a spot smaller that1 mm (near to the diffraction limit).

Figure 24 shows the result of the corresponding experiment, or rather in our case *simulated experiment,* for the generation of the chosen supersonic FW in Fig.23 (still disregarding attenuation). The annular aperture (with radius $R = 35$ mm) is located on the left side of Fig.24, at z = 0. The parameters of the simulation are $N_r = 101$ rings, again with $f = 2.5$ MHz, and $L = 30$ mm. The simulated experiment results to be rather satisfactory. All this does indicate that the

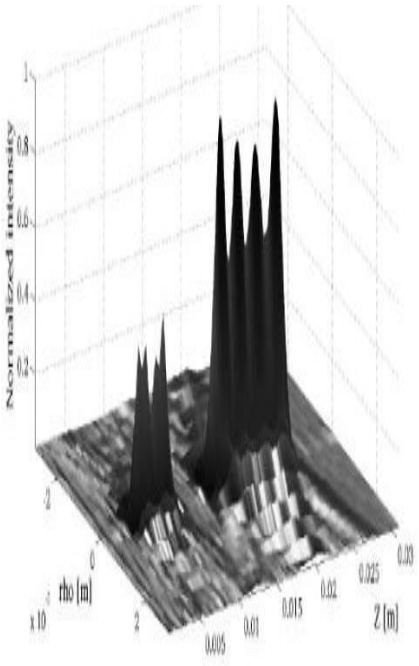

Fig. 24 -- Result of the supersonic *simulated experiment* aimed at constructing the FW appearing above in Fig.23. The annular aperture (with radius $R = 35$ mm) is located on the left side, at z = 0. Axis ρ represents the transverse cylindrical co-ordinate, while z is the longitudinal one. The parameters of the simulation are: $N_r = 101$ rings, again with $f = 2.5$ MHz, and $L = 30$ mm. The simulated experiment results to be rather satisfactory.

experimental generation of non-diffracting beams, and more specifically, of FWs is a real possibility also in the ultrasonic region.

B. Ultrasonic non-diffracting beams or pulses

Let us eventually come to the main issue of this Section 4, which regards the creationof non-diffracting ultrasonic beams, or pulses, having in mind particularly the detection from a distance ofterrestrial mines, or even their explosion.

Two problems are to be faced:

(i) the strong attenuation in air of the ultrasonic waves. We saw in the previous Sections that, e.g, for the 100 kHz frequency, the attenuation is 2 dB/m, implying a quite short depth of field (2 m). We saw it even for a Bessel beam in the air;

(ii) the large power required for such purposes. Indeed, it is relatively easy to work outtransducers for medical applications (imaging, etc.), but it is a considerablechallenge to generate very highpower ultrasound.

Happily enough we can always obtain ultrasonic beams, resisting for long distances both diffraction and attenuation,

by generalizing the method of ours for FWs [20,4,2] (our standard method for FWs is briefly summarized in the Appendix, for convenience of the reader). Let us recall all that by exploiting here one more example of the type examined in Section 2 above.

One more Example (the Fourth)

Similarly to what it was done in Section 2, let us now choose:

1. Frequency: 100 kHz
2. Attenuation coefficient in air: 2 dB/m
3. Depth of field of a normal beam (plane wave or gaussian beam) = 2.2 m

Requested field depth for the FW beam: 10 m
Radius of the desired spot: 5 cm
Needed aperture radius: 0.35 m
Longitudinal intensity pattern chosen: Of the "two steps" type in 0<z<10m

Our theoretical method[20,4,2] allows us to construct an acoustic Frozen Wave with such characteristics, as Figs.25 do show.

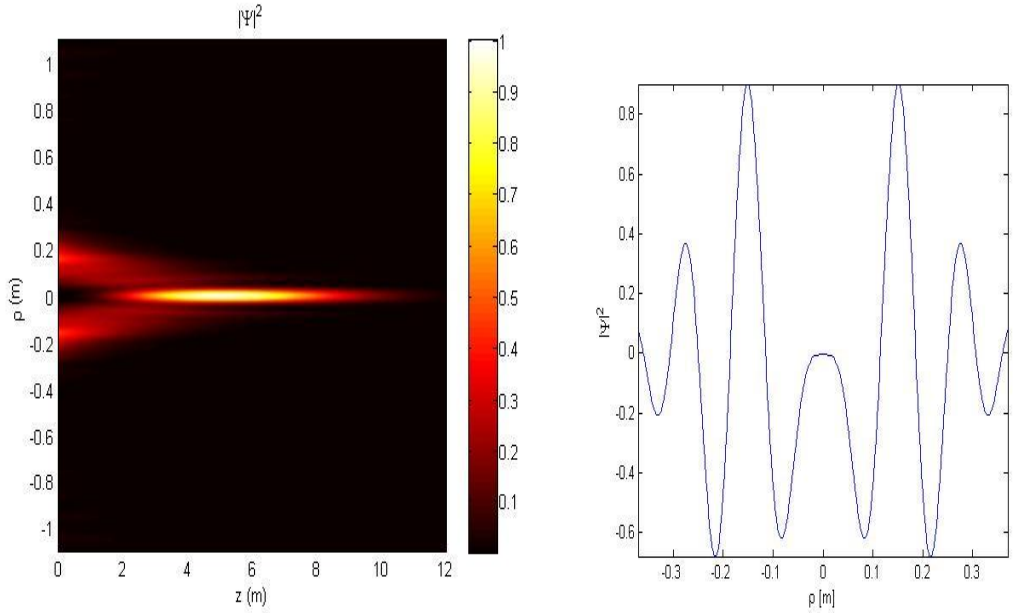

(25 a)(25 b)

Fig. 25 – Our theoretical method[20,4,2] allows constructing an acoustic Frozen Waves with the characteristics specified in the *Example* above. This is shown in the present Figure.

The theoretical possibility of obtaining ultrasonic beams, resisting the effects of diffraction and attenuation for distances very much longer than the ones attained by ordinary beams[4], is rather encouraging. But, let us repeat, the high-power needed for the desired applications, is often a serious obtacle.

In the case of the (last) Example above, one needs an array of annular transducers much bigger than the ones for medical applications.... In Fig.26 we show a possible discretization: It is rather simple, but in it each point represents an annular transducer with at least 1 cm of thickness.

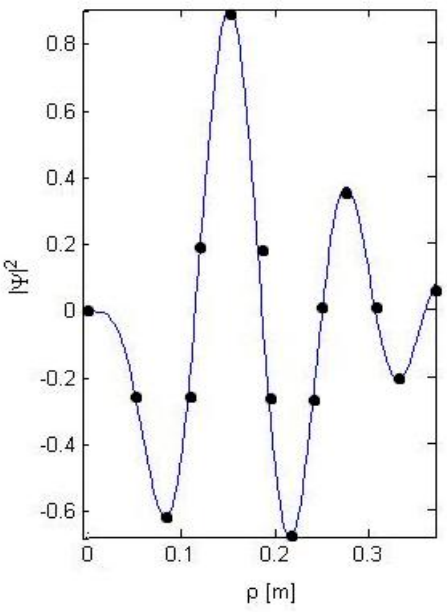

Fig. 26 – For the (last) example above, represented by Figs.25, we can suggest the discretization[9,13] appearing in this Figure: A very simple discretization, but in it each point indicates an annular transducer with at least 1 cm of thickness.

V. BRIEF MENTIONOF SOME AVAILABLE TECHNOLOGY FOR THE GENERATION OF HIGH-POWER ULTRASOUND

Among the existing technologies, let us mention one which seems to be well developed, and has been presented in a series of papers: We confine ourselves here toquoting the work[22] by Gallego-Juarez *et al*. (appeared in 2010 in*Ultrasonics Sonochemistry* **17**, pp.953-964). They showed therein, for instance, how ultrasonic transducers of high-power can be constructed with large radiation areas, and with a design reducing non-linear effects and unwanted modal interactions. A basic structure for such transducers consists of a piezoelectric vibrator which drives a radiator. The vibrator is a sandwich of piezoelectric elements.The vibration caused by the piezoelectric elements is amplified by a mechanical amplifier, causing the radiator to vibrate in one of its modes. Such a radiator may have different geometries, varying with the application; in general, it can be circular or rectangular. Its surface can be moreover modeled, by furrows or bulges, so to get increased control on the radiated field (avoiding mode couplings, etc.), For examples of circular transducers operating in the 10--40 kHz region the interested reader can consult ref.[22]. The simple *circular radiators* considered therein are indeed useful for creating common ultrasonic beams, as the gaussian one; and may be sufficient also for a Bessel beam (when higher order modes are excited, which implies, however, also higher frequencies).

For more complex beams resisting diffraction and attenuation, like the FWs, more sophisticated arrays of high-power transducers are needed.

A. Possible arrays of (high-power) radiators for ultrasonic beams resisting diffraction and attenuation

We have seen that an efficient way for generating non-diffracting beams is the use of an array of annular transducers.

Next, we suggest for instance the use of *sets* of annular radiator arrays, by respecting (see below) annular symmetry; each constituent array being of the *circular* type considered e.g. in the mentioned ref.[22]: See Fig.27. In this Figure the radius of the set of radiators may be, e.g., of about 60--80 cm, while each radiator may have a diameter of 10--15 cm.

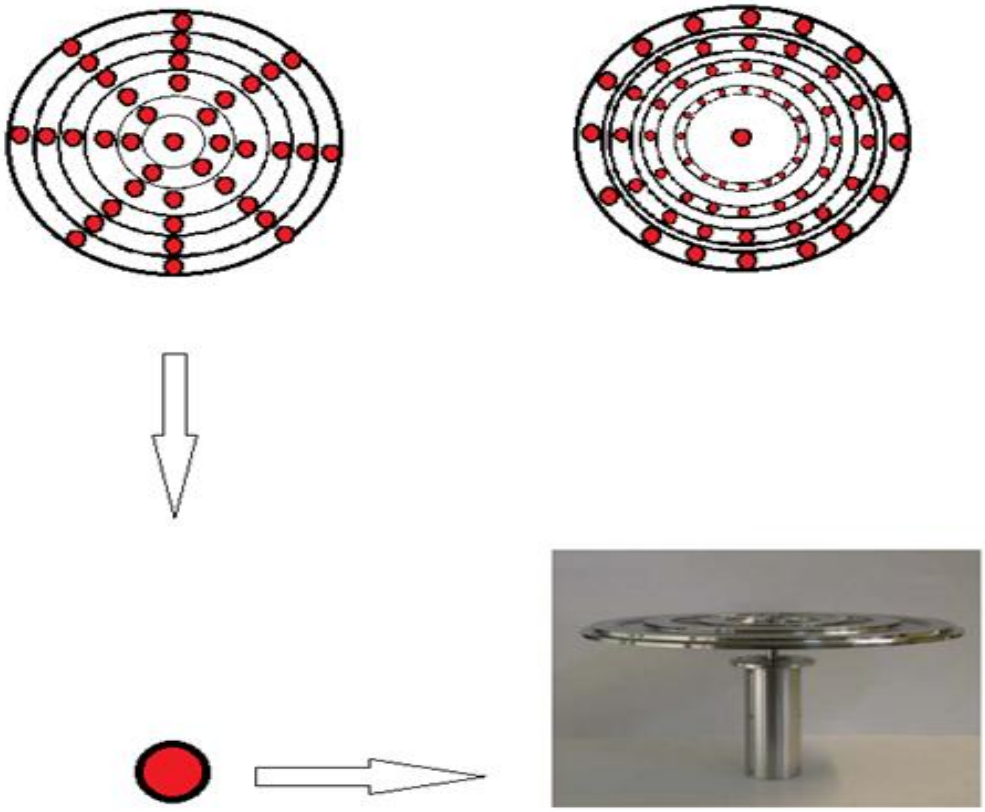

Fig. 27 – For the generation of more sophisticated non-diffracting beams, let us now suggest for instance the use of *sets* of annular radiator arrays, by respecting annular symmetry: See the Figure, where each constituent array is of the *circular* type considered e.g. in the mentioned ref.[22]. The global radius of the set of radiators may be, e.g., of about 60--80 cm, while each radiator may have a diameter of 10--15 cm.

A further possibility is discretizing the annular radiators via the introduction of rectangular (or bended) radiator elements. *Notice* that the excitation to be used for each radiating element canbe obtained from the exact analytic solution which describes, for example, the chosen Frozen Wave. Many more considerations can be found in refs.[1,2] and [13,9].

B. A brief APPENDIX

For possible convenience, let us here summarize (only) a standard method of ours for obtaining the Frozen Waves[17-20]. As we know, it was elsewhere extended for

absorbing media (see, e.g, ref.[20,2]), in order to get FWs resisting both attenuation and diffraction.

Basically, the idea is to obtain non-diffracting beams whose desired longitudinal intensity pattern, $|F(z)|^2$, in the interval $0 \leq z \leq L$, can be chosen a priori. To obtain the desired beam we consider the following solution, given by a superposition of 2N + 1 co-propagating and equal frequency Bessel beams of order ν :

$$\Psi(\rho,\phi,z,t) = e^{-i\omega t}\sum_{n=-N}^{N} A_n J_\nu(k_{\rho n}\rho)e^{ik_{zn}z}e^{i\nu\phi} \tag{10}$$

where $k_{\rho n}^2 = \omega^2/c^2 - k_{zn}^2$ and (with the choice $k_{zn} = Q + 2\pi n/L$) the parameter Q is a constant obeying $0 \leq Q \pm (2\pi/L)N \leq \omega/c$.

In Eq. (1), the coefficients An are given by

$$A_n = \frac{1}{L}\int_0^L F(z)e^{-i\frac{2\pi}{L}nz}dz \tag{11}$$

where $|F(z)|^2$ is the desired longitudinal intensity pattern in the interval $0 \leq z \leq L$. This longitudinal intensity pattern can be concentrated (as we wish) over:

a) the propagation axis ($\rho = 0$). In this case $\nu = 0$ in eq.(10), i.e., we deal with a zero-order Bessel beam superposition. We can also choose the spot radius, $\Delta\rho_0$, of the resulting beam by making $Q = (\omega^2/c^2 - 2.4^2/\Delta\rho_0^2)^{1/2}$; or

b) a cylindrical surface. In this case we deal with $\nu > 0$ values, and the radius ρ_0 of the cylindrical surface can be approximately evaluated through the equation

$$\left(\frac{d}{d\rho}J_\nu\left(\rho\sqrt{\omega^2/c^2 - Q^2}\right)\right)\Bigg|_{\rho=\rho_0} = 0 \tag{12}$$

VI. Acknowledgments

Work partially supported by CAPES (Brazil). The authors thank Massimo Balma, and José L. Prego-Borges, for their stimulating cooperation over the years, and Ioannes M. Besieris for a very helpful critical reading. They acknowledge the continuous useful interest of P. Cardieri, P.L. Dias Peres, and particularly of W. de FreitasFilho and Hugo E. Hernández-Figueroa. Thanks for kind collaboration and interest are also due to RogerL.Garay-Avendano, G.Giardini, DorinaDevona, Claudio Poggi, P.Riva, C.Rizzi, Tarcio A.Vieira and particularly S. Paleari.

References

[1] *Localized Waves*, ed. by H.E.Hernandez-Figueroa, M.Zamboni-Rached, and E.Recami (J.Wiley; New York, 2008), ***book*** of 386 pages.
[2] *Non-Diffracting Waves,* ed. by H.E.Hernandez-Figueroa, E.Recami, and M.Zamboni-Rached (J.Wiley-VCH; Berlin, 2014), ***book*** of 507 pages.
[3] J.L.Prego-Borges, M.Zamboni-Rached, H.E.Hernandez-Figueroa and E.Recami: "Producing Acoustic Frozen Waves: Simulated Experiments", *IEEE Trans. Ultrason. Ferroel.. Freq. Control* **60** (2013) 2414-2425[DOI: 10.1109/TUFFC.2013.6644744].
[4] J.L.Prego-Borges, M.Zamboni-Rached, E.Recami, and E.Tavares Costa: "Producing acoustic 'Frozen Waves': Simulated experiments with diffraction/attenuation resistant beams in lossy media",*Ultrasonics***54** (2014) 1620-1630[DOI: 10.1016/j.ultras.2014.03.008].
[5] Lu-I J.-y. Lu and J.F.Greenleaf: "Nondiffracting X-waves: Exactsolutions to free-space scalar wave equation and their finiteaperture realizations", *IEEE Transactions in UltrasonicsFerroelectricity and Frequency Control***39** (1992) 19-31.
[6] Lu2 J.-y. Lu and J.F.Greenleaf: "Experimental verification ofnon-diffracting X-waves", *IEEE Transactions in UltrasonicsFerroelectricity and Frequency Control***39**(1992) 441-446.
[7] E.Recami, M.Zamboni-Rached, K.Z.Nobrega, C.A.Dartoraand H.E.Hernandez-Figueroa: "On the Localized SuperluminalSolutions to the Maxwell Equations", *IEEE Journal of Selected Topics in Quantum Electronics***9** (2003) 59-73.
[8] E.Recami and M.Zamboni-Rached: "Localized Waves: A Review", *Advances in Imaging & Electron Physics (AIEP)***156** (2009) 235-355 [121 printed pages].
[9] M.Z.Rached, E.Recami and M.Balma: "Simple and effective method for the analytic description of important optical beams when truncated by finite apertures",*Applied Optics***51** (2012) 3370-3379[DOI 1559-128X/12/163370-10].
[10] M.Z.Rached, E.Recami and M.Balma: "A simple analyticalmethod for describing important optical beams truncated by finite apertures", *Progress in Electromagnetics Research, Symposium (PIERS) Proceedings*, Moscow, Russia, Aug. 2012; pp.464-468 [ISSN 1559-9450].
[11] E.Recami, M.Z.Rached, M.E.H.Figueroa, and L.Ambrosio: ``Non-Diffracting Waves: An introduction", Chapter 1 of the book in ref.[2].
[12] M.Zamboni-Rached: "Analytic expressions for the longitudinal evolution of nondiffracting pulses truncated by finite apertures",*Journal of the Optical Society of America* **A23** (2006) 2166-2176.
[13] M.Zamboni-Rached, and E.Recami, "Parabolic antennas, and Circular Slit Arrays, for the generation of Non-Diffracting Beams of Microwaves", arXiv:1408.5635 [physics-optics] (e-print posted in the Archives on Aug. 24, 2014, downloadable from http://arxiv.org/abs/1408.3635).
[14] F.Gori, G.Guattari, and C.Padovani: "Bessel-Gauss beams",*Optics Commun.* **64** (1987) 491-495.
[15] A.O.Barut, G.D.Maccarrone, and E.Recami: "On the Shape ofSuperluminal objetcs",*NuovoCimento***A71** (1982) 509-533.
[16] J.y. Lu: " 2D and 3D high frame rate imaging with limited diffraction beams", *IEEE Trans. Ultrason. Ferroelec. Freq. Control* **44**(1997) 839-856.
[17] M.Zamboni-Rached: "Stationary optical wave fields with arbitrary longitudinal shape by superposing equal frequency Bessel beams: Frozen Waves", *Optics Express***12** (2004) 4001-4006.
[18] M.Zamboni-Rached, E.Recami and H.E.Hernandez-Figueroa: "Theory of `Frozen Waves' " [e-print physics/0502105], *Journal of the Optical Society of America***A11** (2005) 2465-2475.
[19] E.Recami, M.Zamboni-Rached, H.E.Hernandez-Figueroa et al.: "Method and Apparatus for Producing Stationary (Intense) Wavefields of arbitrary shape", **Patent**, application no. US-2011/0100880-A1, publication date 05/05/11; the sponsor having been "Bracco Imaging, Spa".[Available c/o http://www.google.com/patents?id=LLLNAQAAEBAJ&printsec=abstract&source=gbs_overview_r&cad=0#v=onepage&q&f=false]
[20] M. Zamboni-Rached, "Diffraction-Attenuation resistant beams in absorbing media", *Optics Express***14** (2006) 1804-1809.
[21] M. Zamboni-Rached, L. A. Ambrosio, H. E. Hernandez-Figueroa, "Diffraction-Attenuation resistant beams: Higher order versions and finite aperture generations", *Applied Optics* **49** (2010) 5861-5869.
[22] J.A. Gallego-Juárez, G. Rodriguez, V. Acosta, E. Riera, "Power ultrasonic transducers with extensive radiators for industrial processing," *UltrasonicsSonochemistry***17** (2010) 953–964
[23] I.M. Besieris, A.Shaarawi: "Paraxial localized waves in free space", *Optics Express* **12** (2004) 2848-2864.